11A.2 THE PRESTORM ENVIRONMENT OF THE 20 MAY 2013 MOORE OKLAHOMA SUPERCELL ESTIMATED FROM WSR-88D AND TDWR RADAR, AND GOES SATELLITE DATA

Robert M Rabin[1], Qin Xu[1], Kang Nai[1,2] ,Steve Albers[3,4], Hongli Jiang[3,4]

[1]NOAA National Severe Storms Lab, Norman, OK USA
[2]Cooperative Institute for Mesoscale Meteorological Studies Norman, OK USA
[3]NOAA/Earth System Research Laboratory/Global Systems Division (ESRL/GSD)
[4]Cooperative Institute for Research in the Atmosphere, Colorado State University, CO USA

1. INTRODUCTION

On May 20th 2013, a violent tornado devastated the Moore area in central Oklahoma about 20-21:30 UTC. An outlook of a significant severe storm outbreak had been issued a few days in advance by the NOAA Storm Prediction Center. The region of central Oklahoma was under a moderate high risk of severe storms on the morning of the 20th. A tornado watch issued about an hour before the storm developed. Based on model forecasts from the morning of the 20th, the greatest risk of violent tornadoes appeared to be in south-central OK. While supercell storms did develop in that area, they did not produce intense tornadoes as was the case further north.

The supercell associated with the Moore tornado appeared to intensify rapidly near a surface boundary as detected on radar and satellite (Figs 1-2). The cloud free area located northwest of the band of higher reflectivity (1800-1900 UTC) suggests a stable boundary layer in that area, and hence a possible baroclinic zone near the boundary. A north-south oriented cloud band appears to develop by 1900 UTC, intersecting the boundary from the south. This pattern is suggestive of a “triple point” where a dryline intersects a front. The propagation speed of several convective elements on radar suggested mid-level level winds exceeding that analysed and forecasted earlier in the day. These observations served as motivation to examine the wind structure of the near-storm environment for unique factors unavailable in the operational analysis. The wind structure will be examined from WSR-88D and TDWR Doppler radar, GOES satellite, surface mesonet data, and available upper soundings. Output from the variational LAPS analysis system developed at the ESRL/GSD, and from a 3-D variational analysis with advanced radar quality control capability developed at the NSSL, will be presented and compared with the operational analysis for this severe weather event.

2. MULTI-SENSOR BASED WIND ANALYSIS SYSTEM

An upgraded version of the radar-based wind analysis system (RWAS) with improved techniques for Doppler velocity dealiasing (Xu et al. 2011, 2013, 2014) has been developed as support for nowcasting severe thunderstorms. A three-step incremental analysis strategy was designed to improve the mesoscale vector wind analysis. The first step analyzes the Velocity Azimuth Display (VAD) vector winds produced at each radar site together with GOES-13 water vapor winds. The second step analyzes surface wind observations from the Oklahoma Mesonet. In the third step, the radar radial velocities were compressed into superobservations at consecutively refined resolution (from 30 km to 10 km) and the background covariance de-correlation length was adjusted adaptively to consecutively refined scale (from 100 km to 50 km). The system has been applied to radial-velocity observations from five operational WSR-88D radars (KTLX, KFDR, KINX, KVNX, KSRX) and one TDWR radar (TOKC) in combination with surface wind observations from Oklahoma Mesonet and GOES water vapor winds to produce vector wind fields for the Oklahoma Moore tornadic storm case on 20 May 2013. The background wind field is from the nearest NOAA Rapid Refresh (RAP) model predictions interpolated in time and space to the analysis grid in a 800× 800x10 km^3 domain centered at the KTLX radar.

The wind analysis was performed from 1910-2130 UTC at 10-minute intervals. The analysis domain and sample coverage of radar velocity data from the lowest elevation scans at 1900 UTC is shown in Fig 3. Radar signals are from clear air (refractivity fluctuations and insects) and precipitation echoes. Note that radar data are not continuous and cover only a portion of the domain.

3. ANALYSIS RESULTS

Wind analyzes at 0.25 km altitude valid at 1900 UTC are shown in Figs. 4a,b from the background (RAP) and RWAS respectively. These figures cover a sub-region of the domain centered on the TOKC radar location. Dealiased radial wind velocities from the 0.5 deg elevation scans of the TOKC and KTLX radars are superimposed on the analysis wind vectors. Center locations of two mature thunderstorms “K1” and “K2”, and a developing cluster of storm cells “E” are labeled in the figures. Cells “K1” and “K2” weaken in the subsequent hour. Rapid development of “E” leads to the Moore tornado by 19:30 UTC. A wind shift or frontal boundary is evident near “E” in both the RAP and RWAS. The RWAS suggests a stronger horizontal wind shear and cyclonic flow in vicinity of “E” with southerly to southeasterly inflow and northwesterly flow to the rear, behind the frontal boundary. The RAP has weak southwesterly winds in that later region.

The wind analyzes are shown over the full domain at 1.5

* *Corresponding author address:* Robert M Rabin, NOAA/National Severe Storms Lab, 120 David l Boren Blvd., Norman, OK 73072; email: bob.rabin@noaa.gov

and 3.0 km altitudes valid at 1900 and 2000 UTC in Figs 5-6. Arrows indication wind direction. Wind speed is given by the color enhanced background. The background wind field (RAP top rows) and the RWAS wind analysis (bottom rows) can be compared in these figures. Given that the GOES satellite-based winds are above 5km altitude, there is no impact of these observations at the heights shown.

At 1.5 and 3.0 km, the local maximum of southwesterly winds in south central Oklahoma appears to be stronger in the RWAS analysis than in RAP forecast. This is especially notable at 3.0 km, where the peak wind speed exceeds 30 m/s, as compared to less than 25 m/s in the RAP. At 3.0 km, the RWAS analysis also suggests a more compact local wind maximum in south central Oklahoma surrounded with stronger horizontal gradients to the west and north. The wind speed pattern resolved in the RAP is more uniform. The band of strongest winds extends north and northeastward through central Oklahoma, in vicinity of the surface boundary. The wind analysis from RWAS suggests stronger 0-3 km shear near, and to the south and east of the discrete thunderstorms.

The relative vorticity at 1900 and 2000 UTC from the corresponding wind analyzes at 3.0 km are shown in Fig. 7. At 1900 UTC, a center of high positive vorticity appears in the general location of storm “K1”. As this echo moves northeast, it passes well south of Moore and nearly dissipates by 2000 UTC. The associated vorticity at 3.0 km also dissipates. A vorticity signature associated with cluster “E” was first detected at 1920 UTC (not shown). By 2000 UTC, the center of maximum vorticity is located in the general location of the tornadic storm in central Oklahoma, however it is displaced at least 30 km to the northwest of the mesocyclone. These vorticity features are not present in the RAP 1-hr forecasts. In the lower levels (0.5 and 1.5 km), significant vorticity was not detected with the storms “K1” and “K2” and did not appear with intensifying Moore storm until 1950 UTC. These results suggest that the multi-sensor wind analysis detected rotation at the mid-levels (3.0 km) on 50-100 km horizontal scales associated with existing thunderstorms. However, there is no evidence of a significant precursor in vorticity prior to storm development or intensification.

The variational LAPS (vLAPS) system, developed at the NOAA/ESRL/GSD, was run in near real-time on 20 may 2013, as part of the Hazardous Weather Testbed (HWT) in Norman OK. A wide range of observational data including WSR-88D radar radial velocity and reflectivity, and GOES satellite data were assimilated into the analysis. The format, resolution, and quality control of the radar data were not identical to those used in the RWAS analysis. Using a diabatic initiation at 1900 UTC, the vLAPS analysis was used to produce forecasts at 1-minute intervals from the WRF model on a 1-km grid. Forecast composite reflectivity between 1900 and 2000 UTC is shown in Fig. 8. The cell “K1” at 1900 UTC did not weaken as observed, but continued to intensify and move south of the Moore area by 2000 UTC. The model did not correctly forecast the intensification of the weaker “E” cells from 1900 to 2000 UTC. The cell “K1” became the dominant storm. The forecast track was at least 30 km south of that of the observed Moore supercell.

4. CONCLUSIONS.

A multi-sensor analysis system (RWAS) was upgraded to perform dealiasing of Doppler radial velocity data and to include GOES atmospheric motion vectors (AMVs) along with surface mesonet wind observations. Data from five WSR-88D, one Terminal Doppler Weather Radar (TDWR), Oklahoma Mesonet sites, and GOES AMVs were used to analyze the mesoscale wind fields during the development and intensification of the supercell thunderstorm associated with the devastating Moore tornado on 20 May 2013. In contrast to the background wind field used as input to the RWAS, the analysis revealed a broad band of stronger winds at about 3 km altitude ahead of the developing storms, suggesting a stronger 0-3 km wind shear in that region. A southward propagating front or wind shift boundary, and cyclonic flow in vicinity of the boundary were detected near the developing storm.

This analysis provides evidence of stronger vertical wind shear than was detected with the RAP model, and the existence of weak cyclonic rotation in vicinity of the southward moving boundary. However, these observations do not provide a definitive theory of the rapid intensification and rotation of the supercell associated with the Moore tornado and the weakening of the cell to its south. Since the variational LAPS incorrectly developed the storm further south, it will be interesting to explore the possible impact of assimilating the RWAS wind analysis on those forecasts in a future study.

5. ACKNOWLEDGEMENTS.

This research was supported by the ONR Grant N000141410281 to the University of Oklahoma (OU). Funding was also provided by DOC/NOAA/OAR under NOAA-OU Cooperative Agreement #NA17RJ1227 and a grant from the GOES-R Risk Reduction Program.

6. REFERENCES.

Xu, Q., K. Nai, L. Wei, P. Zhang, S. Liu, and D. Parrish, 2011: A VAD-based dealiasing method for radar velocity data quality control. *J. Atmos. Oceanic Technol.*, **28**, 50–62.

Xu, Q., K. Nai, S. Liu, C. Karstens, T. Smith and Q. Zhao, 2013: Improved Doppler velocity dealiasing for radar data assimilation and storm-scale vortex detection. *Advances in Meteorology*. **2013**, Article ID 562386, 10 pages (517–526).

Xu, Q., L. Wei, K. Nai, S. Liu, R. Rabin, and Q. Zhao, 2014: A Radar Wind Analysis System for Nowcast Applications. Submitted to *Advances in Meteorology*.

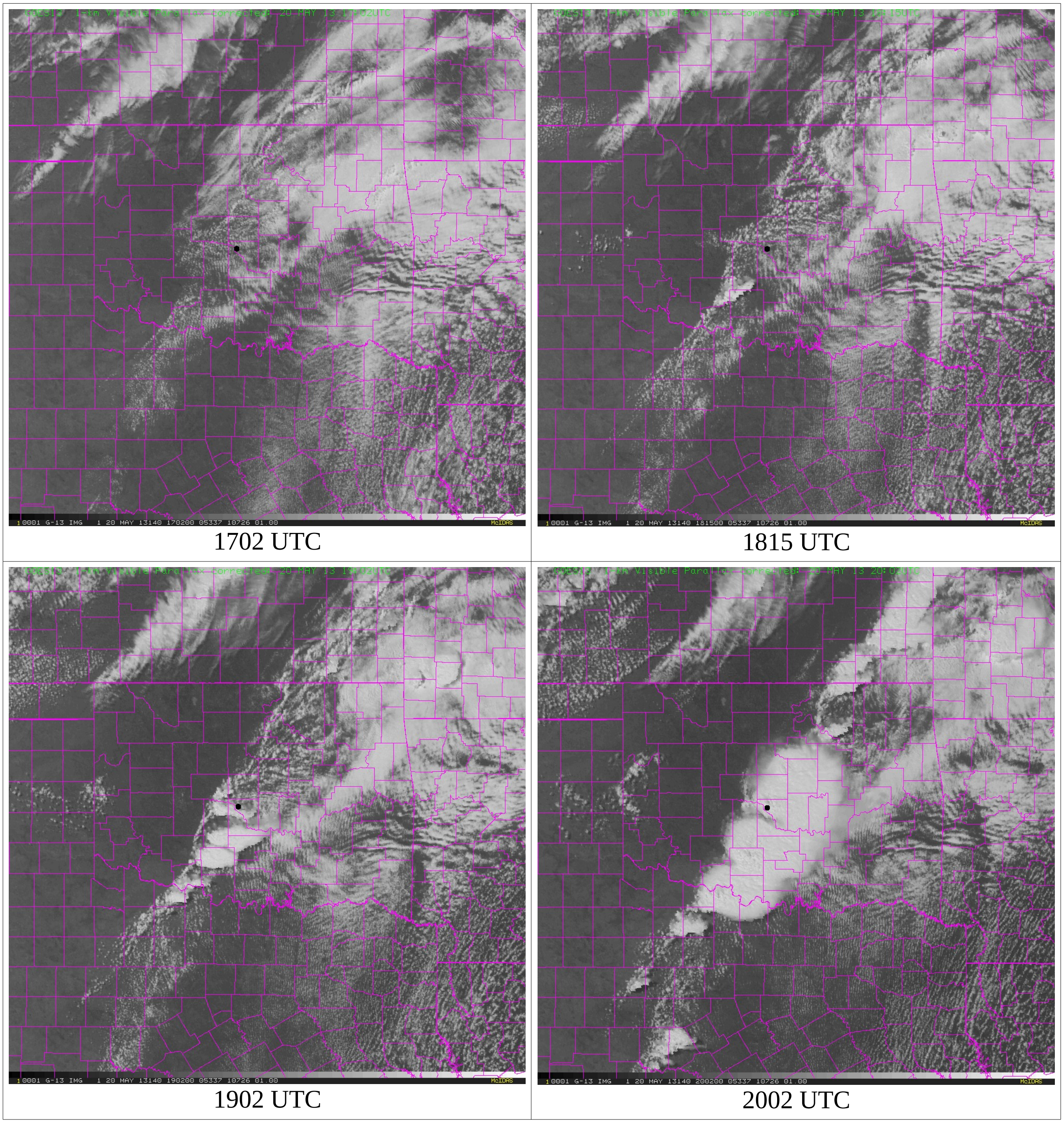

Fig. 1. Visible satellite imagery from GOES-13 at 1702, 1815, 1902, 2002 UTC. An algorithm was applied to adjust locations of each cloud pixel to account for parallax displacement using cloud top temperature from infrared imagery. Location of TOKC radar indicated by black dot. County and state boundaries shown in cyan.

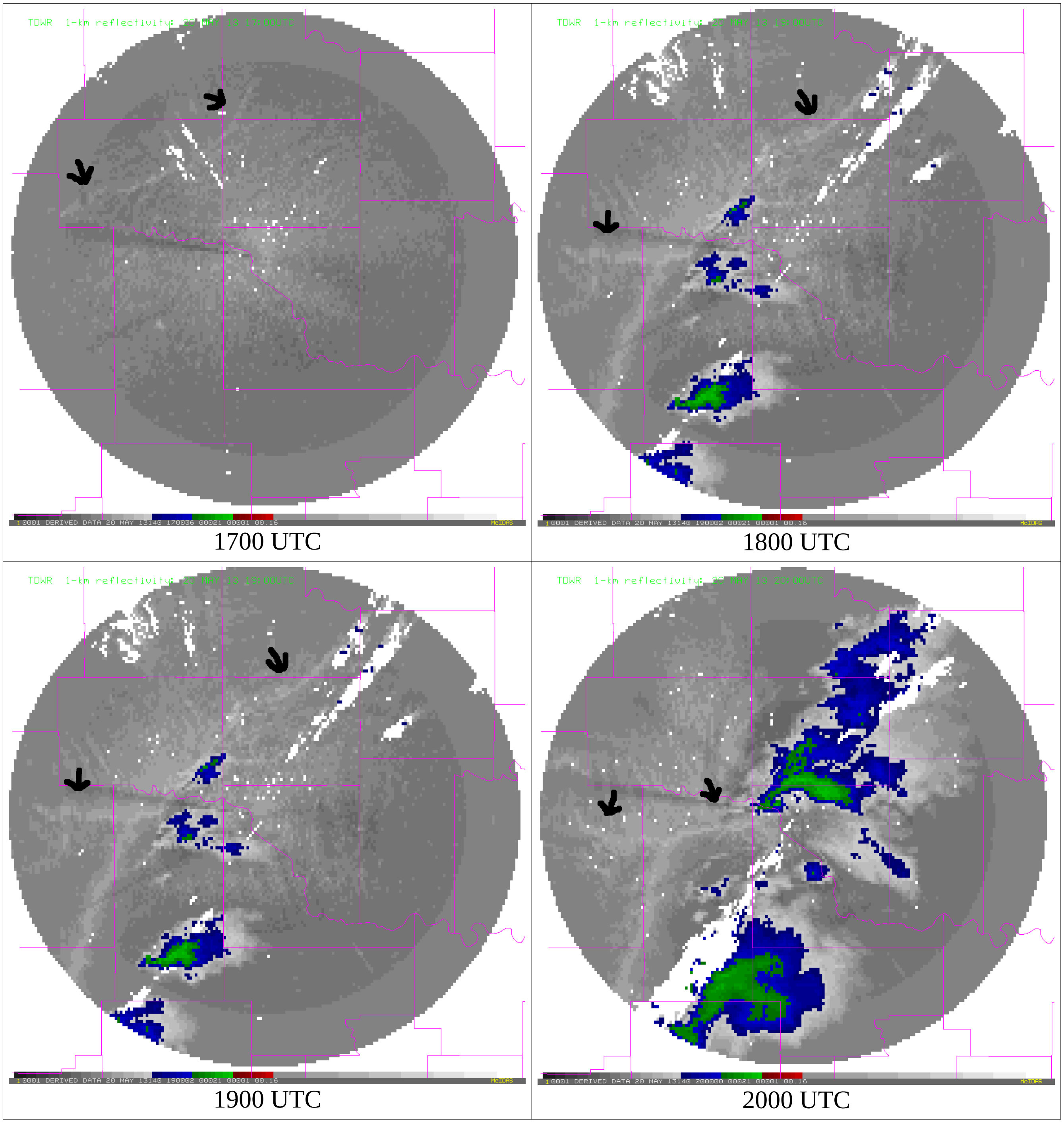

Fig. 2. Radar reflectivity scans at 0.5 deg elevation from FAA Terminal Doppler radar (TOKC) located in Norman OK (approximate 10 km south of Moore, OK) at 1700, 1800, 1900, 2000 UTC. Location of apparent southward moving boundary indicated by arrows.

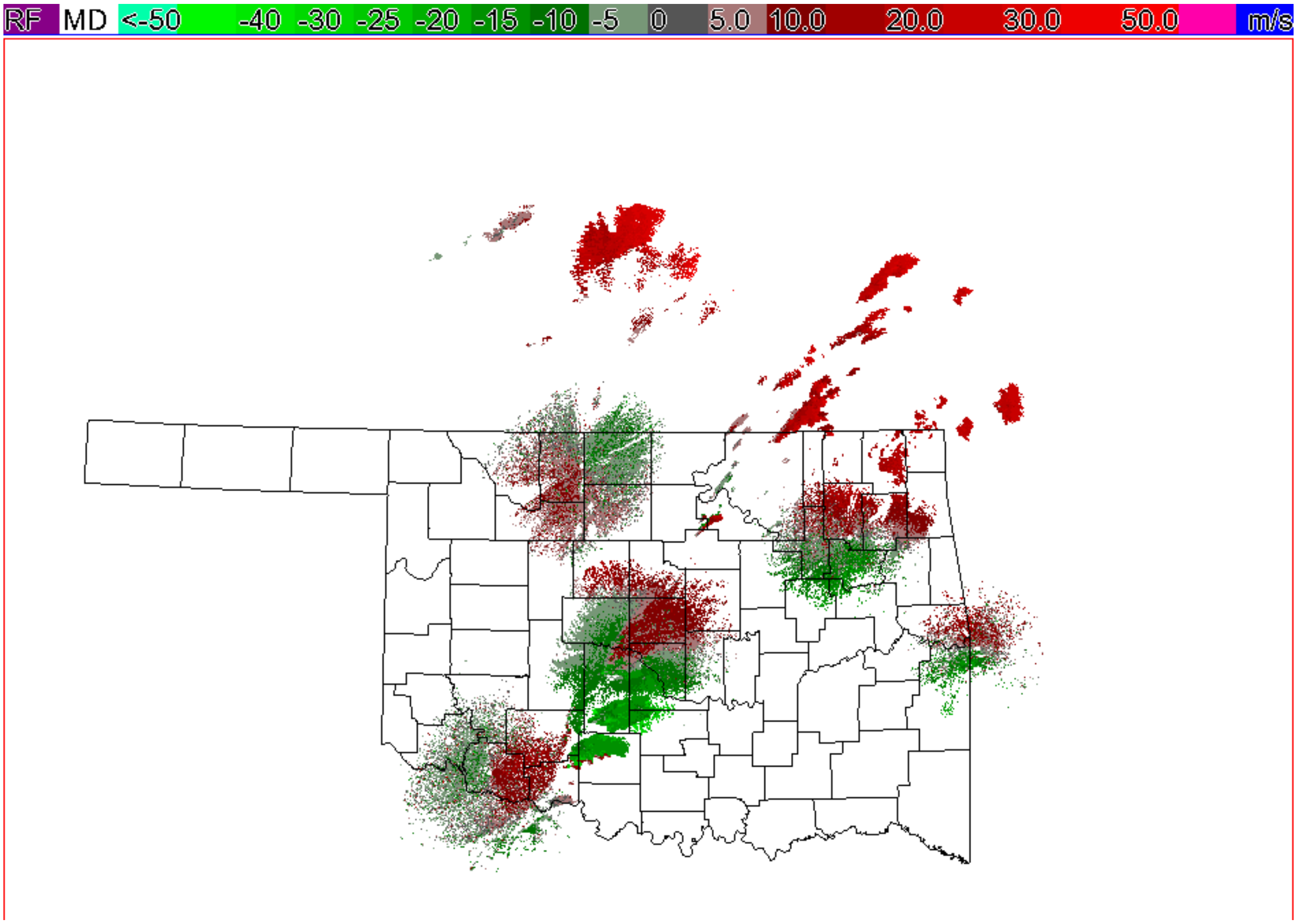

Fig. 3. Radial velocities at 0.5 deg elevation angles from available Doppler radars. 20 May 2013, 1900 UTC. Red are outbound (green are inbound) velocities relative to each individual radar.

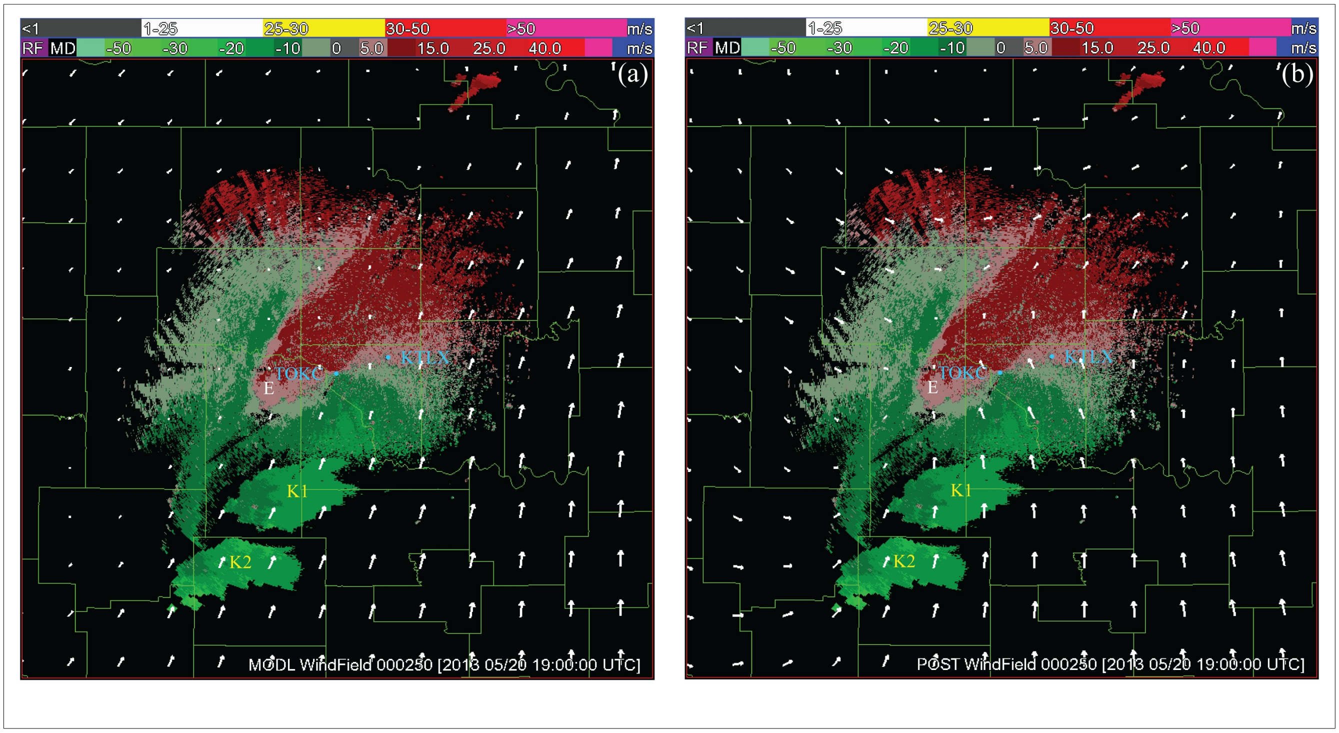

Fig. 4: Analyzed winds at grid points on 0.25 km altitude surface valid at 1900 UTC: a) RAP, b) RWAS. Grid points are separated by 20 km. Doppler radial velocity data from lowest elevation TOKC and KTLX radar scans are superimposed. County boundaries shown in light green. Storm cells K1,K2,E indicated (see text).

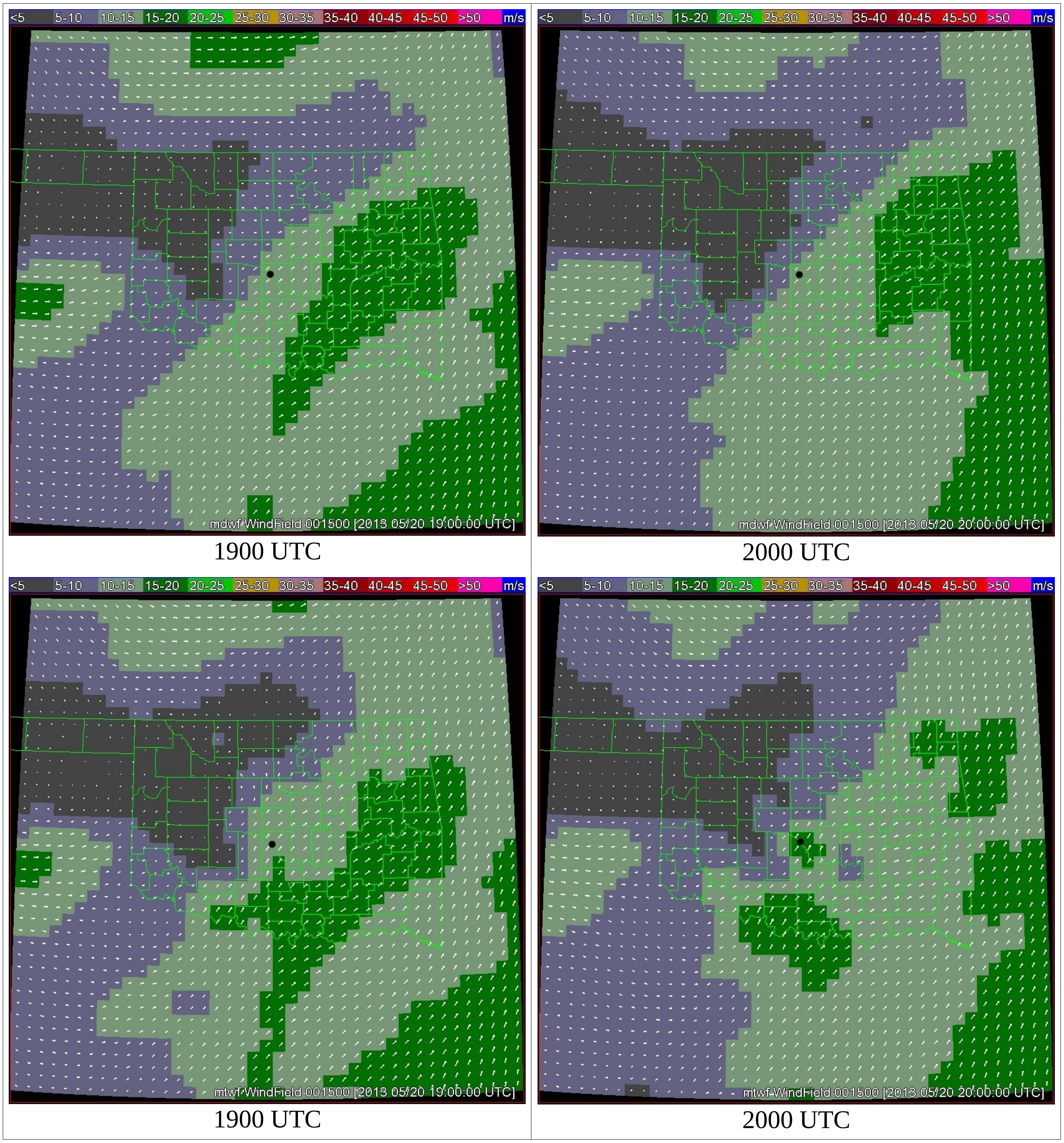

Fig. 5. Wind direction and speed at 1.5 km altitude: 1900 UTC (left column) and 2000 UTC (right column). Upper row is 1-hr RAP forecast. Bottom row is from the RWAS analysis. State and county boundaries in Oklahoma shown in light green. Location of TOKC radar indicated by black dot.

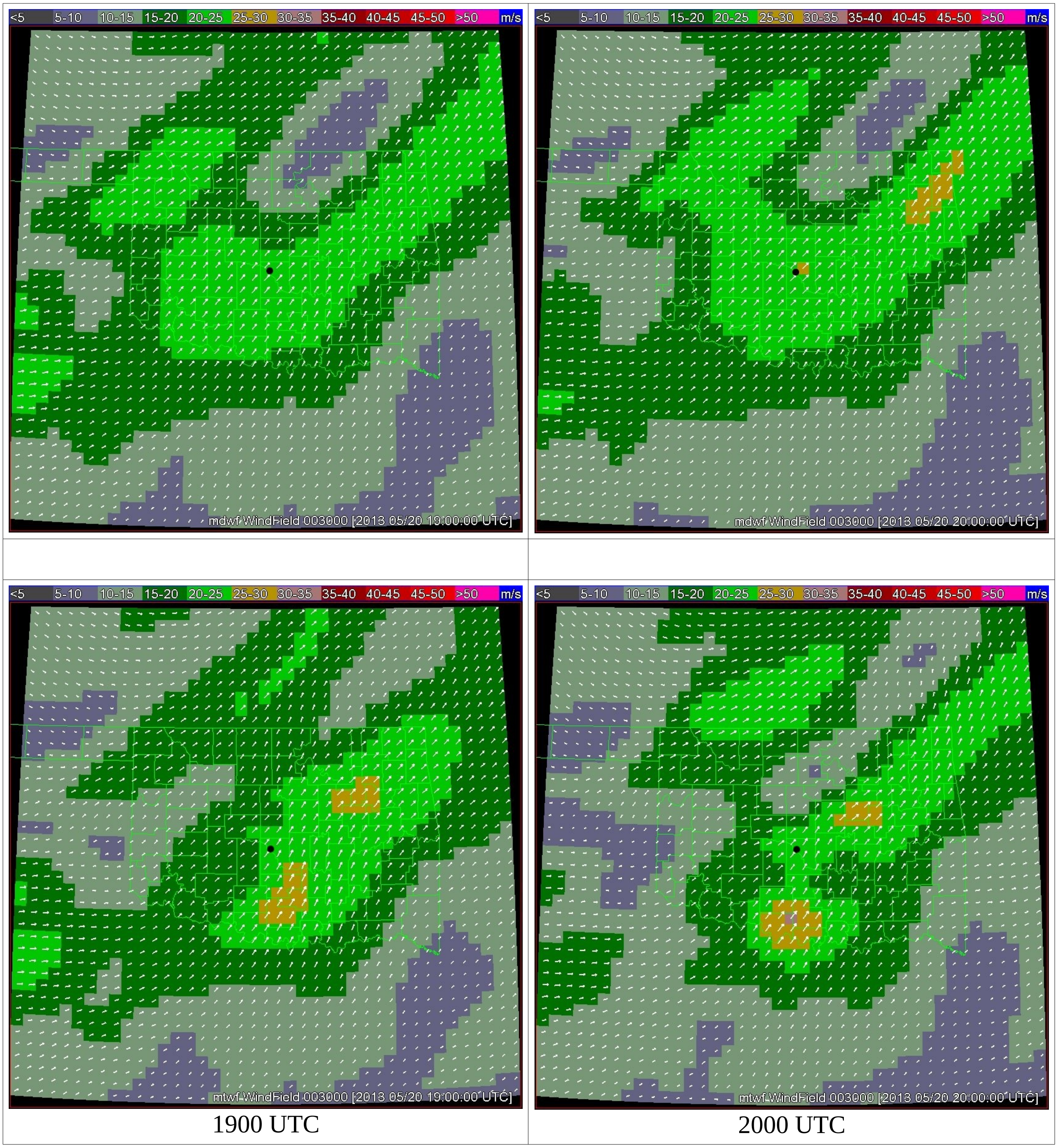

Fig. 6. Wind direction and speed at 3.0 km altitude: 1900 UTC (left column) and 2000 UTC (right column). Upper row is 1-hr RAP forecast. Bottom row is from the RWAS analysis. State and county boundaries in Oklahoma shown in light green. Location of TOKC radar indicated by black dot.

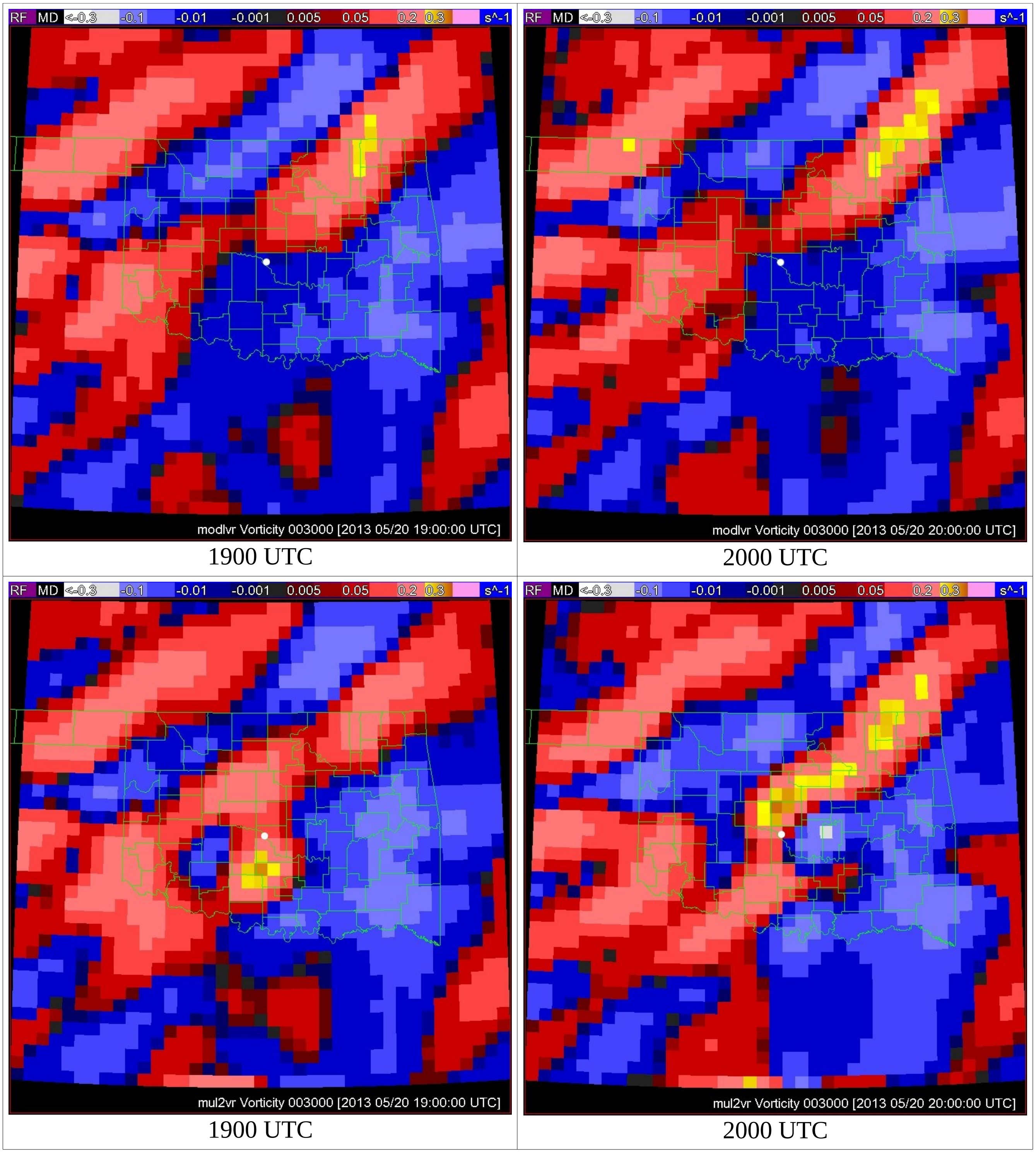

Fig. 7. Vorticity at 3.0 km altitude: 1900 UTC (left column) and 2000 UTC (right column). Upper row is 1-hr RAP forecast. Bottom row is from the Multi-sensor analysis. State and county boundaries in Oklahoma shown in light green. Location of TOKC radar indicated by white dot.

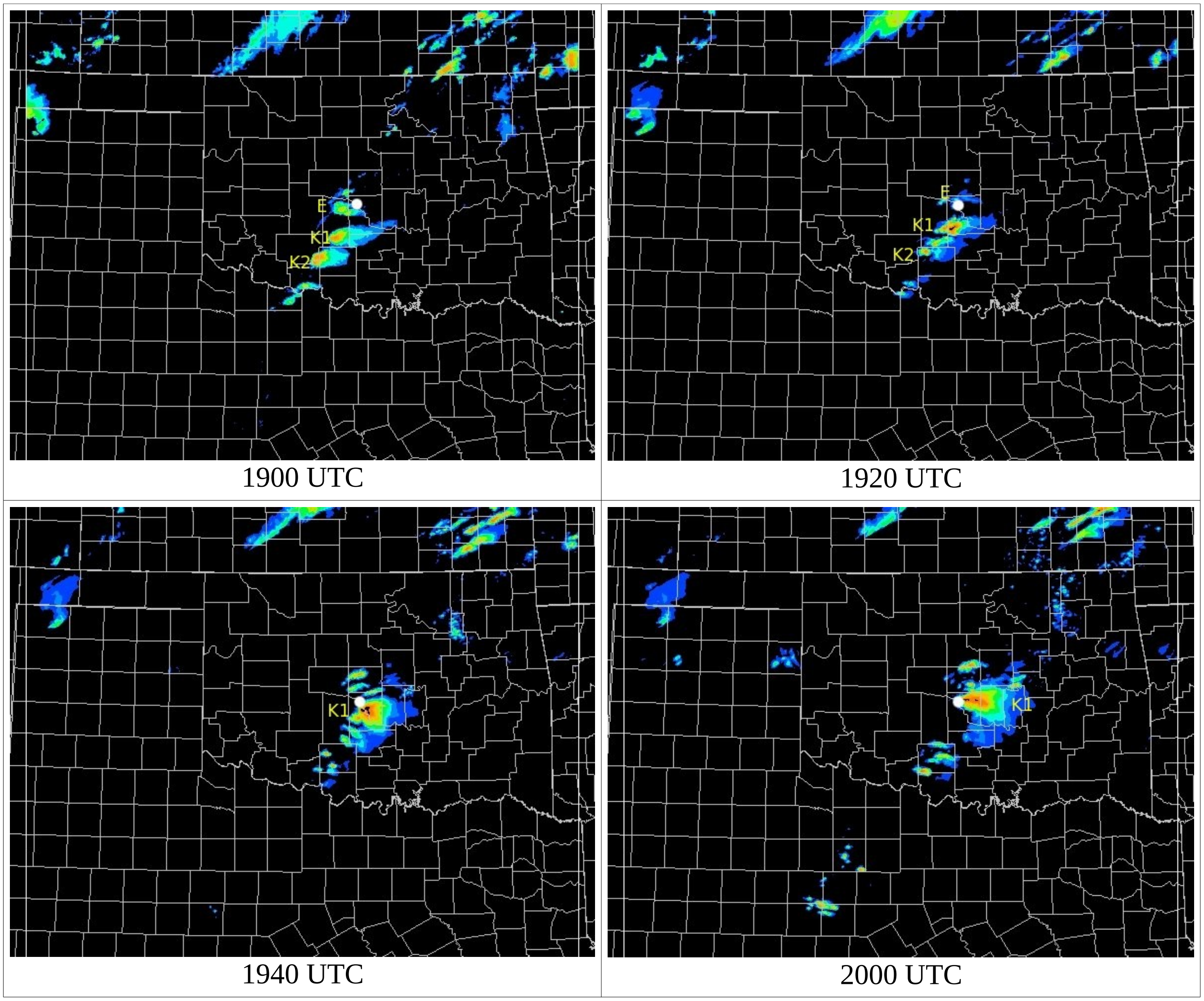

Fig. 8. Forecast composite reflectivity from the variational LAPS model: 1900, 1920, 1940, 2000 UTC. Location of TOKC radar is indicated by white dots. Labels of storms refer to those in Fig. 4.